Available online at www.sciencedirect.com
SCIENCE DIRECT®
ELSEVIER
Journal of Magnetism and Magnetic Materials 286 (2005) 18–22
Journal of magnetism and magnetic materials
www.elsevier.com/locate/jmmm

Epitaxial growth and magnetic properties of Fe nanowedge islands on Mo(1 1 0)

V. Usov, S. Murphy*, I.V. Shvets

SFI Laboratory, Physics Department, Trinity College, College Green, Dublin 2, Ireland

Available online 12 October 2004

Abstract

Fe films with a nominal thickness $\geqslant 2$ Å grown on Mo(1 1 0) at $500 \leqslant T \leqslant 750$ K self-assemble into nanowedge islands supported on a pseudomorphic Fe wetting layer. We discuss mechanisms that contribute to the island growth and distribution. Fe adatoms migrate towards the islands under the influence of the strain induced in the substrate around each island and subsequently enter the island through a vertical climb mechanism. We demonstrate that the magnetic properties of these nanostructures are governed by their shape and do not display the in-plane spin reorientation transition found in the morphologically similar Fe/W(1 1 0) system.
© 2004 Elsevier B.V. All rights reserved.

PACS: 68.37.Ef; 68.55.Ac; 75.75.+a; 81.16.Dn

Keywords: Self-assembly; Iron; Molybdenum; STM; SMOKE

Scanning tunneling microscopy (STM) studies of the Fe/Mo(1 1 0) epitaxial system have shown that under elevated growth conditions, the Fe films self-assemble into nanowedge islands supported on a pseudomorphic wetting layer [1–3]. The shape of these nanowedge islands is the result of surface energy minimisation. Their sides are typically aligned along low-index crystallographic directions and they maintain a flat (1 1 0) surface that remains unbroken by steps, though the island may cross several substrate terraces. As a result, the local thickness of the island may vary from a few atomic layers at one end to several tens of layers at the other. Similar structures have been obtained by depositing Fe, Cu, Ni and Ho on W(1 1 0) [4–7] and Pb on Si(1 1 1) [8]. In this study, we explore mechanisms that contribute to the nanowedge self-assembly in the Fe/Mo(1 1 0) system and show how they are linked to the mismatch-induced strain. We have also investigated the magnetic properties of these nanostructures in-situ using surface magneto-optical Kerr effect (SMOKE) measurements.

*Corresponding author. Tel.: +353 1 6082020; fax: +353 1 6083228.
E-mail address: shmurphy@tcd.ie (S. Murphy).

0304-8853/$ - see front matter © 2004 Elsevier B.V. All rights reserved.
doi:10.1016/j.jmmm.2004.09.028

The sample preparation and analysis were performed in ultra-high vacuum (UHV). To extract the general features of the nanowedge formation and their magnetic properties two Mo substrates were used, with miscuts of 0.65° and 4.6° from the (1 1 0) plane, respectively. The first had an average terrace width of ~ 200 Å and monatomic steps aligned along the [1 $\bar{1}$ $\bar{1}$] crystal direction. The second had an average terrace width of ~ 25 Å with monatomic steps oriented perpendicular to the [1 $\bar{1}$ $\bar{1}$] direction. Each substrate was cleaned by annealing in 5×10^{-7} Torr O_2 at $1300 \leqslant T \leqslant 1500$ K for 30–60 min cycles, followed by flash-annealing several times to 2400 K for 10–15 s in UHV. Fe films were deposited by e-beam evaporation of a 3N purity Fe rod at rates of 0.005–0.01 Å s^{-1}.

Because of the much larger terrace width on the low-index surface, it was easier to extract details of the initial stages of nanowedge formation on this surface by STM. The first Fe layer and up to 80% of the second layer form nanowires by the step-flow growth mechanism at 500 K [2]. The first Fe layer is a pseudomorphic wetting layer that is stable to 800 K [9]. However, dislocations are formed along the [0 0 1] direction in second layer nanowires above a critical wire width of ~ 100 Å [2]. Fe adatoms nucleate along these dislocations to form third layer protrusions as shown in Fig. 1a, indicating that the enhanced binding energy for adatoms at these sites [2] plays an important role even at these elevated temperatures. When the protrusions on successive terraces overlap and coalesce, small nanowedges are formed (Fig. 1b). This is accompanied by a roughening of the step-edges as the second Fe layer breaks up and is absorbed into the nanowedges.

We propose that the localised strain field produced in the substrate around each of these nanowedges helps it to soak up the adatoms in its vicinity. To illustrate this point, we performed a finite element calculation on the simple model of a 1 nm thick Fe disk bonded to a Mo substrate. The diameter of the disk is in the range of 10–100 nm, while the thickness and diameter of the substrate are 1000 and 2000 nm, respectively. The Fe disk is isotropically strained to reflect the 9% lattice mismatch and in this expanded state it is bonded

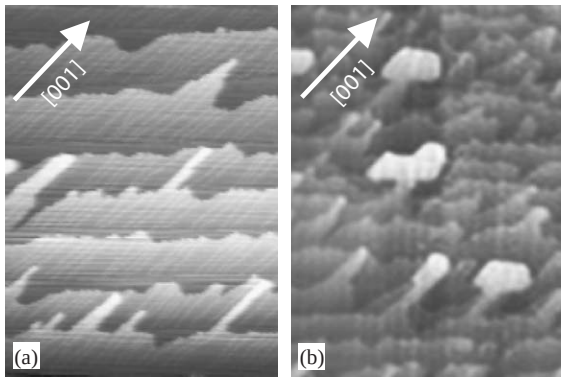


Fig. 1. 260 × 350 nm STM images of a film with 3 Å nominal thickness grown on the low-index Mo(1 1 0) surface at 495 ± 15 K. (a) Fe protrusions form along dislocations in the second Fe layer. (b) Protrusions on successive layers overlap and coalesce to form nanowedges. The second layer breaks up and is absorbed by these islands.

to the substrate. We use the stress–strain relation $\sigma = C(\varepsilon - \varepsilon_0)$, where ε_0 stands for the initial strain of the disk. The strain vector is given by

$$\begin{pmatrix} \varepsilon_r \\ \varepsilon_\theta \\ \varepsilon_z \\ \gamma_{rz} \end{pmatrix} = \begin{pmatrix} \dfrac{\partial u}{\partial r} \\ \dfrac{u}{r} \\ \dfrac{\partial w}{\partial r} \\ \dfrac{\partial u}{\partial z} + \dfrac{\partial w}{\partial r} \end{pmatrix}, \tag{1}$$

where r, z, θ are the coordinates of the cylindrical system, u and w are the radial and axial displacements, respectively, and are both independent of θ. The stiffness tensor

$$C = \frac{E}{(1+v)(1-2v)} \times \begin{pmatrix} 1-v & v & v & 0 \\ v & 1-v & v & 0 \\ v & v & 1-v & 0 \\ 0 & 0 & 0 & \dfrac{1-2v}{2} \end{pmatrix} \tag{2}$$

includes Youngs' modulus E and Poisson's ratio v for the isotropic material. We use E values of 211×10^9 (SI Units) and 329×10^9 (SI Units) and v values of 0.33 and 0.293 for Fe and Mo,

respectively. As the Fe disk relaxes inwards, it produces a tensile radial strain and compressive circumferential strain in the substrate surface outside its perimeter. Fig. 2 shows the dependency of the radial strain component $\varepsilon_r = \partial u/\partial r$ at the substrate surface as a function of the distance from the centre of disks of different sizes. As one would expect intuitively, islands of greater size create larger strained areas in the substrate.

Recent atomic scale calculations for Co islands on Cu(1 1 1) have demonstrated that the Co islands induce an anisotropic strain in the substrate in their vicinity [10]. This strain influences the adatom diffusion in the vicinity of the island, since the adatom binding energy and adatom diffusion barrier show a dependency on the surface strain. For compressive strain the diffusion barrier is reduced, while for low tensile strain ($\leqslant 4\%$) it is increased and for large tensile strain it decreases again [11]. In the Fe/Mo(1 1 0) system, the pseudomorphic Fe wetting layer already accommodates a large tensile strain (9%). This strain is increased further in the vicinity of an island, lowering the diffusion barrier so that adatoms will diffuse towards the island. As the size of the strained area depends on the island size, larger islands soak adatoms from a larger surrounding area, which is reflected by a greater separation between larger islands in the STM data.

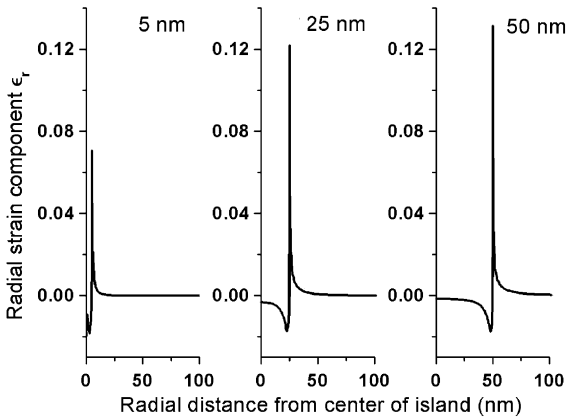


Fig. 2. Calculated radial strain profile in a Mo substrate covered by 1 nm thick Fe disks of 5, 25 and 50 nm radii, respectively. The tensile strain drops to 1% of its maximum value at approximately 9, 18 and 22 nm from the edge of the 10, 50 and 100 nm diameter disks, respectively.

Upon reaching a nanowedge, the adatoms must undertake a vertical climb up each side of the island. We propose that dislocations in the lower layers of the nanowedge act as diffusion channels to facilitate this vertical climb mechanism. The sites where dislocations thread to the walls of the island produce regions of compressive strain, which trap adatoms that diffuse along the edges of the island. The growth of the wedge shape of the islands can be assisted by two mechanisms. First, more adatoms are soaked up from the substrate by the thicker end of the nanowedge because it produces a larger strain in the substrate. Second, for adatoms that have reached the island, the diffusion barrier is lowered towards the thick end. This is because the film lattice is relaxed by the introduction of dislocations, which switches the strain to the regime where the adatom diffusion barrier decreases as the tensile strain is reduced [11]. Adatoms deposited on the (1 1 0) surface of the island diffuse to the edges of the island where they are incorporated through exchange and this gives rise to the characteristically flat surface.

Longitudinal SMOKE measurements were performed in-vacuum at room temperature on these nanostructures. The films were typically deposited at room temperature and post-annealed at 750 K to form the nanowedge islands. For films grown at room temperature, the film morphology is characterised by layer-by-layer growth up to two atomic layers, above which there is a switch to Stranski–Krastanov growth. These films display a uniaxial anisotropy with the easy axis of magnetisation along the [0 0 1] direction (cf. Fig. 3d) for coverages down to nearly two atomic layers. Below this coverage, the Curie temperature of the films lies below room temperature. A step-induced anisotropy was found in films grown on the vicinal surface at room temperature [12].

Fig. 3a shows an example of nanowedges grown on the vicinal surface. The high step density produces an elongation of the islands along the direction of the step edges. This produces a shape anisotropy, which is superimposed on the magnetocrystalline anisotropy of the films and slightly shifts the easy axis of magnetisation from the [0 0 1] direction towards the step edge direction. This shape anisotropy is absent in the case of

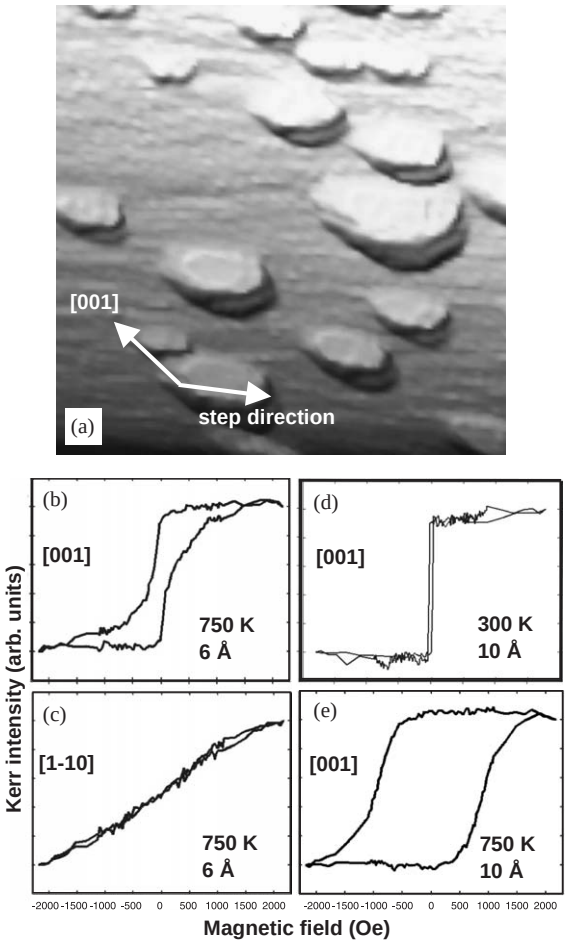


Fig. 3. (a) 200×200 nm STM image of nanowedge islands grown on vicinal Mo(1 1 0) by depositing 4.5 Å Fe at 300 K and annealing to 750 K. The islands are up to ~ 30 Å thick at their thick ends. (b) and (c) Kerr loops taken along the [0 0 1] and [1 $\bar{1}$ 0] directions, respectively, for a 6 Å film grown at 750 K. (d) and (e) Easy axis Kerr loops taken for 10 Å Fe films grown at 300 K and 750 K, respectively.

nanowedges grown on the low-index surface, which grow preferentially along the [0 0 1] direction [2]. Otherwise, there is no evidence of step-induced anisotropy in nanowedges grown on either the vicinal or low-index surface. For films grown at both 300 and 750 K on both substrates, the magnetic easy axis lies along the [0 0 1] direction (neglecting step-induced or shape anisotropies), while the hard axis lies along the [1 $\bar{1}$ 0] direction (Figs. 3b–e). By comparison, in the Fe/W(1 1 0) system, films grown at room temperature display a surface anisotropy that orients the magnetic easy axis along the in-plane [1 $\bar{1}$ 0] direction. Upon annealing these films, the magnetic easy axis reorients to the in-plane [0 0 1] direction due to the bulk anisotropy coming from the Fe nanowedges. Therefore, the Fe/Mo(1 1 0) system does not display the in-plane spin reorientation transition observed for the morphologically similar Fe/W(1 1 0) system [13]. Comparing Figs. 3d and e, it is clear that the nanowedge films display higher coercivity and saturation fields than their counterparts grown at 300 K. This is attributed to the demagnetising field associated with the shape of the nanowedges. The demagnetising field is higher for thicker nanowedges, which have a larger vertical aspect ratio, resulting in a higher coercivity in thicker films (cf. Figs. 3b and d). The importance of magnetostatic energy in this type of nanostructure has recently been demonstrated for Fe nanowedges grown on W(1 1 0) using spin-polarised STM [14]. These nanowedges display a thickness-dependent domain configuration, starting as single domains in islands with a local thickness of up to 35 Å. For the Fe/Mo(1 1 0) films studied here, the nominal deposited thickness would suggest that the nanowedges form single domains, with the possible exception of the 10 Å films grown on the vicinal surface, where the nanowedges are up to 40–50 Å thick and may have a more complex domain structure.

This work was supported by the Science Foundation Ireland under contract 00/PI.1/C042.

References

[1] J. Malzbender, M. Pryzbylski, J. Giergiel, J. Kirschner, Surf. Sci. 414 (1998) 187.
[2] S. Murphy, D. Mac Mathúna, G. Mariotto, I.V. Shvets, Phys. Rev. B 66 (2002) 195417.
[3] J. Osing, I.V. Shvets, Surf. Sci. 433–435 (1999) 440.
[4] H. Bethge, D. Heuer, C. Jensen, K. Beshöft, U. Köhler, Surf. Sci. 331–333 (1995) 878.
[5] K. Reshöft, C. Jensen, U. Köhler, Surf. Sci. 421 (1999) 320.
[6] C. Schmidthals, D. Sander, A. Enders, J. Kirschner, Surf. Sci. 417 (1998) 361.
[7] G. Piaszenski, R. Göbel, C. Jensen, U. Köhler, Surf. Sci. 454–456 (2000) 712.

[8] I.B. Altfeder, K.A. Matveev, D.M. Chen, Phys. Rev. Lett. 78 (1997) 2815.
[9] M. Tikhov, E. Bauer, Surf. Sci. 232 (1990) 73.
[10] D.V. Tsivlin, V.S. Stepanyuk, W. Hergert, J. Kirschner, Phys. Rev. B 68 (2003) 205411.
[11] H. Brune, K. Bromann, H. Röder, K. Kern, J. Jacobsen, P. Stoltze, K. Jacobsen, J. Nørskov, Phys. Rev. B 52 (1995) R14380.
[12] V. Usov, S. Murphy, I.V. Shvets, J. Appl. Phys. 95 (2004) 7312.
[13] D. Sander, A. Enders, C. Schmidthals, D. Reuter, J. Kirschner, Surf. Sci. 402–404 (1998) 351.
[14] M. Bode, A. Wachowiak, J. Wiebe, A. Kubetzka, M. Morgenstern, R. Wiesendanger, Appl. Phys. Lett. 84 (2004) 948.